Received: 30 July 2020 | Accepted: 6 November 2020

DOI: 10.1002/hyp.13973

WOMEN ADVANCING RESEARCH IN HYDROLOGICAL PROCESSES

WILEY

Fingerprinting hydrological and biogeochemical drivers of freshwater quality

Ann Louise Heathwaite[1] | Magdalena Bieroza[2]

[1]Lancaster Environment Centre, Lancaster University, Lancaster, UK

[2]Department of Soil and Environment, Swedish University of Agricultural Sciences, Uppsala, Sweden

Correspondence
Magdalena Bieroza, Department of Soil and Environment, Swedish University of Agricultural Sciences, Uppsala 75007, Sweden.
Email: magdalena.bieroza@slu.se

Funding information
Natural Environment Research Council, Grant/Award Number: NE/G001707/1; Stiftelsen Lantbruksforskning, Grant/Award Number: O-16-23-640; Svenska Forskningsrådet Formas, Grant/Award Number: 2018-00890

Abstract

Understanding the interplay between hydrological flushing and biogeochemical cycling in streams is now possible owing to advances in high-frequency water quality measurements with in situ sensors. It is often assumed that storm events are periods when biogeochemical processes become suppressed and longitudinal transport of solutes and particulates dominates. However, high-frequency data show that diel cycles are a common feature of water quality time series and can be preserved during storm events, especially those of low-magnitude. In this study, we mine a high-frequency dataset and use two key hydrochemical indices, hysteresis and flushing index to evaluate the diversity of concentration-discharge relationships in third order agricultural stream. We show that mobilization patterns, inferred from the hysteresis index, change on a seasonal basis, with a predominance of rapid mobilization from surface and near stream sources during winter high-magnitude storm events and of delayed mobilization from subsurface sources during summer low-magnitude storm events. Using dynamic harmonic regression, we were able to separate concentration signals during storm events into hydrological flushing (using trend as a proxy) and biogeochemical cycling (using amplitude of a diel cycle as a proxy). We identified three groups of water quality parameters depending on their typical *c-q* response: flushing dominated parameters (phosphorus and sediments), mixed flushing and cycling parameters (nitrate nitrogen, specific conductivity and pH) and cycling dominated parameters (dissolved oxygen, redox potential and water temperature). Our results show that despite large storm to storm diversity in hydrochemical responses, storm event magnitude and timing have a critical role in controlling the type of mobilization, flushing and cycling behaviour of each water quality constituent. Hydrochemical indices can be used to fingerprint the effect of hydrological disturbance on freshwater quality and can be useful in determining the impacts of global change on stream ecology.

1 | INTRODUCTION

High-frequency monitoring of freshwaters with in situ sensors enables collection of hydrochemical data at time scales matching those of hydrological, biological and chemical dynamics observed in streams (Kirchner et al., 2004). This unprecedented technological breakthrough enables us to address fundamental questions about how stream ecosystems function, including process understanding of

dominant hydrochemical and stream metabolic regimes (Bernhardt et al., 2018; Burns et al., 2019). Insights regarding the stream hydrochemical regime and the interplay between hydrological and biogeochemical processes are encapsulated in the concentration-discharge (*c-q*) relationship and can be interrogated for high and low flows with the aid of high-frequency measurements.

During high flows and under hydrological flushing, the downstream transport of solute and particulate material dominate (Boyer et al., 1997; Burns, 2005), and high-frequency measurements enable the detection of hysteresis responses indicating changes in solute/particulate mobilization and delivery. Several studies have attempted to quantify storm event *c-q* responses by designing hydrochemical indices to describe the direction of the hysteresis loops and their magnitude; with hysteresis and flushing indices being the most popular (Butturini et al., 2008; Lloyd et al., 2016a). Although several relationships were reported between the *c-q* indices and potential controlling factors (Aubert et al., 2016; Bieroza & Heathwaite, 2015; Moatar et al., 2017), we lack a systematic understanding of how different hydrological and biogeochemical processes contribute to the observed hydrochemical patterns.

During low flows, when biogeochemical cycling in freshwaters dominates, high-frequency measurements enable detection of diel and sub-daily cycles in hydrochemical time series. Diel cycles are driven by diurnal changes in light, temperature, redox potential, stream metabolism (production and respiration), uptake/release, denitrification/nitrification, evapotranspiration and bioturbation (Hensley & Cohen, 2016; Nimick et al., 2011; Smolders et al., 2017). Owing to the dependency of biogeochemical processes on temperature, diel cycles are most pronounced during spring and summer, with lower amplitudes in winter (Burns et al., 2016; Halliday et al., 2012). The change in amplitude of diel cycles expresses the intensity of biogeochemical processes and is often used to derive an estimation of their rates, for example, for stream metabolism (Bernhardt et al., 2018) and nutrient assimilation (Rode, Halbedel Nee Angelstein, et al., 2016).

The interplay between hydrological and biogeochemical processes at different spatial scales (horizontal from hillslopes to riparian zone and vertical from groundwater to hyporheic zone) is controlled by catchment properties including water travel times and the rates of biogeochemical processes responsible for retention, mobilization and delivery of solutes and particulates to the stream network (Ameli et al., 2017; Ensign & Doyle, 2006; Wollheim et al., 2018). The land-stream interface of the riparian and hyporheic and zones are areas of particularly dynamic and spatially-variable interactions between hydrological and biogeochemical processes (Johnes et al., 2020; Lewandowski et al., 2020). Generally, the presence of an abundant source of solute in the catchment, for example, agricultural land use for nutrients (Banwart, 2011; Heathwaite, 2010) and bedrock for weathering solutes (Beerling et al., 2020), creates an internal loading that reduces the diversity in the stream *c-q* responses and increases the frequency of chemostatic behaviour with increasing stream order (Basu et al., 2011; Godsey et al., 2009, 2019). However, anthropogenic solutes (nutrients) can show highly variable *c-q* responses from strong dilution to strong concentration, and the inter-catchment variability is often larger than within-catchment temporal variability due to different geological substrates and depths of solute generation (Botter et al., 2020). Much research has focused on headwater catchments because they are thought to be locations in the stream network where hydrological flushing-biogeochemical cycling and chemostatic-chemodynamic responses are potentially in balance, according to the River Continuum conceptual framework (Vannote et al., 1980): there is growing evidence from catchment studies to support this hypothesis (Abbott et al., 2018; Bieroza et al., 2018; Creed et al., 2015; Lynch et al., 2019; Wollheim et al., 2018).

Our understanding of temporal drivers of the interplay between hydrological and biogeochemical processes is continually evolving with intense focus on the analysis of changes in seasonal drivers (temperature and storm event magnitude) and inter-storm variation in solute biogeochemical retention and its effect on flushing behaviour (Burns et al., 2019). Seasonality was found to play an important role in controlling the *c-q* responses of phosphorus and turbidity, with winter chemostatic-clockwise and summer chemodynamic-anticlockwise storm events in a groundwater-fed river system (Bieroza & Heathwaite, 2015). Seasonal *c-q* patterns were found to differ from event-based ones for phosphorus and nitrate in 219 French catchments covering a wide range of soil, climate and land use characteristics (Minaudo et al., 2019). These differences between long-term and event-based *c-q* responses likely indicate different controls on solute transport and storage processes on different temporal scales (Knapp et al., 2020). More recently, the notion that biogeochemical cycling is switched off or severely dampened, depending on the magnitude of the storm event has gained prominence, with higher magnitude storm events thought to have a greater damping effect (Bernhardt et al., 2018; Raymond et al., 2016) compared to low-magnitude storm events that can preserve diel cycles (Burns et al., 2016).

Despite this wealth of information on *c-q* patterns at high and low flows thanks to advances in high-frequency measurements, our understanding of the interplay between hydrological flushing and in-stream biogeochemical cycling remains limited. The existing studies tend to focus on either flushing during storm events or cycling during low flows. Here, we aim to advance the understanding of the interplay between flushing and cycling during storm events for multiple parameters and hydrological years. We use high-frequency hydrochemical data to evaluate the variability in storm *c-q* patterns and seek to partition and understand the discrete contributions from hydrological flushing and biogeochemical cycling. For the purpose of this study we assume that these two processes operate separately over the short timescales of individual storm events (here on average 17 hours), and that both contribute to the observed solute and particulate *c-q* signals. We base our analysis on the calculation of hydrochemical indices (i.e. the hysteresis and flushing indices) for whole and decomposed (into underlying trend and diel component) concentration time series. We synthesise our findings into a conceptual framework of solute and particulate hydrochemical behaviour under storm events of varying magnitude for a third order agricultural catchment in a groundwater-fed river system that has been the focus of detailed research on hyporheic zone processes (Binley et al., 2013; Heppell et al., 2013; Lansdown et al., 2015) and a broader study of the entire river Eden catchment (Ockenden et al., 2016; Reaney et al., 2019).

2 | MATERIALS AND METHODS

2.1 | Study catchment and hydrochemical data

The River Leith in situ automated laboratory (2009–2014) provided measurements of total phosphorus (TP), total reactive phosphorus (TRP), turbidity (TURB), nitrate nitrogen (NO_3-N), dissolved oxygen (DO), specific conductivity (COND), redox potential (RED), pH and water temperature (TEMP) for unfiltered stream water samples on an hourly basis. TP and TRP measurements were carried out by the wet-chemistry analyser (Systea's Micro Mac) with the remaining parameters analysed using Systea's WaterWatch instrument. The details of the experimental setup can be found in (Bieroza et al., 2014, 2018). Continuous 15-min stream stage, flow discharge and meteorological data were obtained from the UK National River Flow Archive (https://nrfa.ceh.ac.uk/, UK Centre for Ecology and Hydrology).

The River Leith catchment (54 km^2, third Strahler order, 2.6°W 54.5°N, rainfall 957 mm, 1999–2014) is dominated by clay loam and silty loam soil textures, is predominantly used for agriculture and has ca. 85% permanent grassland cover. The study site near Cliburn has been the subject of detailed reach scale evaluation of physical hydrology (Binley et al., 2013), nitrogen dynamics (e.g., Krause et al., 2009) and water quality with in situ sensing (Bieroza & Heathwaite, 2015, 2016). The River Leith is a sub-catchment to the river Eden basin (2400 km^2), where the predominantly chemostatic stream export of nutrients, particularly N, is controlled by the legacy stores within the Penrith Sandstone (Wang & Burke, 2017). Such chemostatic response reflects large mass legacy stores that buffer the variability in concentrations (Thompson et al., 2011) and integrate, for example, the long-term increases in nitrate concentrations observed in the sandstone aquifer of the Eden catchment. There is potential for legacy N to accumulate in the stream network over time, which may obscure hydrochemical indices with increasing stream order. Previous work suggests that in the third order River Leith, there remains a dynamic equilibrium between chemostatic and chemodynamic responses (Bieroza et al., 2014, 2018; Bieroza & Heathwaite, 2015).

2.2 | Data processing and analyses

Hourly water quality data were collated, checked for outliers and temperature-corrected. The data are expressed as values at 25°C for DO, COND and RED. The quality of the dataset was assured by cross-checking with routine (weekly) grab samples and also comparison with monitoring data independently collected by the UK Environment Agency (http://environment.data.gov.uk/water-quality).

Flow discharge data (15 min interval) were used to identify discrete storm events in two steps. The first step used identification of events with flow discharge above 0.3 m^3s^{-1}, starting at the first time with an increase in flow of 10% in 1 hr and finishing at the first time with a decrease of 1% following the approach of (Dupas et al., 2016). The second step involved analysis of the flow discharge first derivative to identify rising and falling limbs as periods with flow above the calibrated threshold values of 0.05 and −0.025 ls^{-2} respectively (Minaudo et al., 2017). The multiple-peak events were identified as single storm events if the flow discharge between individual peaks had not dropped by more than 50% and if the gap between them was less than 3 hrs. For each storm event, a number of characteristics were calculated including duration of the event, duration of the rising and falling limb, maximum flow discharge, flow discharge volume during the event, time from the previous storm event, time to the next storm event and a 5 day antecedent precipitation index (API_5; Equation (1), Tables 1 and S1) (Brocca et al., 2008). We classified storm events according to their magnitude using a single Q_{max} threshold of 1.7 m^3s^{-1}, resulting in 80 high-magnitude (average Q_{max} = 13.2 m^3s^{-1}) and 74 low-magnitude (average Q_{max} = 0.72 m^3s^{-1}) storm events respectively. We only examined storm events with >70% data completeness for all tested parameters.

To evaluate the effect of each storm event on water quality parameters, each dataset was divided into three periods: (1) before storm event (BF), (2) during storm event (ST) and (3) after storm event (AF), with ST corresponding to the storm event identified as above and BF and AF being actual times from the previous and to the next storm event. In cases where BF and AF were longer than 30 hrs, a fixed time of 30 hrs was used.

Two empirical indices were calculated to describe *c-q* responses during storm events: hysteresis index (H_i; Equation (2), Table 1) and flushing index (F_i; Equations (3) & (4), Table 1). The hysteresis index describes the concentration change on the rising and falling limbs of the storm event hydrograph: $H_i < -0.1$ anticlockwise response—concentrations on the falling limb are higher than on the rising limb, $-0.1 < H_i < 0.1$ linear response, $H_i > 0.1$ clockwise response—concentrations on the rising limb are higher than on the falling limb. H_i can be calculated for any percentile of flow during the storm event and typically the 50th percentile (H_{i_50}) is chosen to represent the index value (Lloyd et al., 2016a). In many instances e.g. from 34% for TEMP to 59% for RED (average for all parameters 42%), it was not possible to calculate the exact H_{i_50} value due to rising and falling limbs covering different flow percentiles. Consequently, we used a mean value of H_i across all available flow percentiles (H_{i_Mean}). The differences between mean H_{i_50} and H_{i_Mean} were not statistically significant (Figure S1).

The flushing index describes a relative change in parameter concentrations during the storm event: $F_i < -0.1$ dilution response—concentrations decrease with the flow, $-0.1 < F_i < 0.1$ neutral response, $F_i > 0.1$ concentration response—concentrations increase with the flow. We observed that F_i, since being based on just two points, was sensitive to the presence of noisy data, multiple-peak storm events and diurnal changes in concentrations (Figure S4) leading to inaccurate representation of flushing behaviour. Therefore, we propose a new calculation of F_{i_Mean}, based on mean concentrations in the period before and during the storm event (Equation (4), Table 1). The differences between mean F_{i_Point} and F_{i_Mean} were not statistically significant with the exception of TURB for which mean F_{i_Mean} was lower than F_{i_Point} (0.46 vs. 0.55; Figure S5). Based on the

TABLE 1 Definition of the key variables and their equations used in the study

Equations	Definition	Description
(1)	$API_5 = kP_2 + k^2P_3 + k^3P_4 + k^4P_5 + P_1$	API_5—a 5 day antecedent precipitation index; k—is a decay parameter here set to 0.95; P_i—sum of precipitation for ith day before the storm event (Brocca et al., 2008)
(2)	$H_{i\_k} = C_{RL\_Qk} - C_{FL\_Qk}$ $H_{i\_Mean} = \left(\sum_{k=0}^{1} H_{i\_k}\right)/n$ $C_{RL\_Qk} = \text{interp}(Q_{RL}, C_{RL}, Qk)$ $C_{FL\_Qk} = \text{interp}(Q_{FL}, C_{FL}, Qk)$ $Q_{RL} = Q_{norm_{RL}}$ $C_{RL} = C_{norm_{RL}}$ $Q_{FL} = Q_{norm_{FL}}$ $C_{FL} = C_{norm_{FL}}$ $C_{norm} = \frac{C - C_{min}}{C_{max} - C_{min}}$ $Q_{norm} = \frac{Q - Q_{min}}{Q_{max} - Q_{min}}$	H_i—hysteresis index (Lloyd et al., 2016b); k—index calculated at 5% flow discharge, between 0 and 1; H_{i_k}—H_i calculated for the kth percentile of flow e.g. H_{i_50} is a H_i calculated for the 50th flow percentile; H_{i_Mean}—H_i calculated as the mean value of all available values of H_{i_k}, n number of all available H_{i_k} values; Q_k—flow calculated for percentile k; C_{RL_Qk}—normalized concentration on the rising limb corresponding to Q_k, calculated as a linear interpolation based on normalized flow and concentrations on the rising limb (Q_{RL} and C_{RL}); C_{FL_Qk}—normalized concentration on the falling limb corresponding to Q_k, calculated as a linear interpolation based on normalized flow and concentrations on the falling limb (Q_{FL} and C_{FL}); Q_{max}—maximum value of Q during storm event; Q_{min}—minimum value of Q; C_{max}—maximum concentration; C_{min}—minimum concentration.
(3)	$F_{i\_Point} = \frac{(C_s - C_b)}{C_p}$	F_{i_Point}—flushing index calculated based on single concentration values, C_s—concentration at the peak of the storm event, C_b—concentration at the baseflow, beginning of the storm event, C_p—the highest of the two values: $C_p = C_s$ if $C_s > C_b$ and $C_p = C_b$ if $C_b > C_s$ (Butturini et al., 2008)
(4)	$F_{i\_Mean} = \frac{(C_{ST} - C_{BF})}{C_p}$	F_{i_Mean}—flushing index calculated based on mean concentration values, C_{ST}—mean concentration for the storm event (ST), C_{BF}—mean concentration for the period before the storm event (BF), C_p—the highest of the two values: $C_p = C_{ST}$ if $C_{ST} > C_{BF}$ and $C_p = C_{BF}$ if $C_{BF} > C_{ST}$
(5)	$y_t = \text{Trend}_t + \text{Seasonal}_t + \text{Short}_t + e_t$	y_t—observed time series, Trend_t—trend component, Seasonal_t—seasonal component, here assumed to be zero due to the short-term duration of individual storm events, Short—cyclical components of period 24, 12, 8 and 6 hr, e_t—error component (Young et al., 1999)

combination of H_i and F_i, nine discrete *c-q* types were defined to describe the behaviour of solutes and particulates during storm events (Figure 1).

To investigate the effect of storm events on hydrological flushing and biogeochemical cycling simultaneously, we decomposed the high-frequency time series into the underlying trend as a proxy for hydrological flushing, and amplitude as a proxy for biogeochemical cycling using Dynamic Harmonic Regression (DHR) as described in Equation (5) in Table 1 (Young et al., 1999). The method is typically used to examine the long-term trends, seasonality and short-term fluctuations in time series, including water quality data (Halliday et al., 2012). The method is also suitable for analysing high-frequency water quality time series since it can handle missing data (Young et al., 1999). Here, we conducted the time series decomposition into the underlying trend and short-term components (periodicity corresponding to 24, 12 and 8 hr components) using the CAPTAIN toolbox (Young et al., 2019). The exact periodicity of the cyclic components was determined with the autoregression model; for the diel component it varied from 21 to 27 hrs. The DHR model estimates the parameters recursively (trend's slope, amplitude and phase of the short-term cyclical components) using the Kalman Filter and the Fixed Interval Smoother (Halliday et al., 2012; Young et al., 1999). The parameters are time-varying, which allows examination of their behaviour before, during and after the storm event. Since the storm event time series are trend dominated, there is a risk of spectral overlap between trend and cyclic components and model overparameterisation. To avoid this, visual inspection of spectrum and decomposed trend and cyclical components was carried out and a single value of Noise Variance Ratio (NVR) hyper-parameter was chosen for all cyclical components to avoid model overfitting (Young et al., 1999, 2019). We focus on the trend and diel component as they explained most of the variance (>90%) in the concentration time series and we assume that they represent hydrological flushing and biogeochemical cycling respectively. To quantify flushing and cycling behaviour, we calculated F_i for trend (F_{i_Trend}) and amplitude (F_{i_Amp}) separately, using Equation (4) in Table 1. Based on this data, we have defined six dominant flushing and cycling responses: (1) concentration effect $F_{i\_Trend} > 0.1$, (2) dilution effect $F_{i\_Trend} < -0.1$, (3) neutral effect (neither concentration nor dilution) $-0.1 \geq F_{i\_Trend} \leq 0.1$; (4) enhancement effect $F_{i\_Amp} > 0.1$, (5) dampening effect $F_{i\_Amp} < -0.1$, and (6) neutral effect (neither enhancement nor dampening) $-0.1 \geq F_{i\_Amp} \leq 0.1$.

To compare the differences in mean concentrations between the parameters, seasons and storm characteristics (Table S1), a non-parametric analysis of variance was used (Kruskal–Wallis test). All data processing and statistical analyses were carried out in MATLAB version 9.4 (MathWorks, 2018).

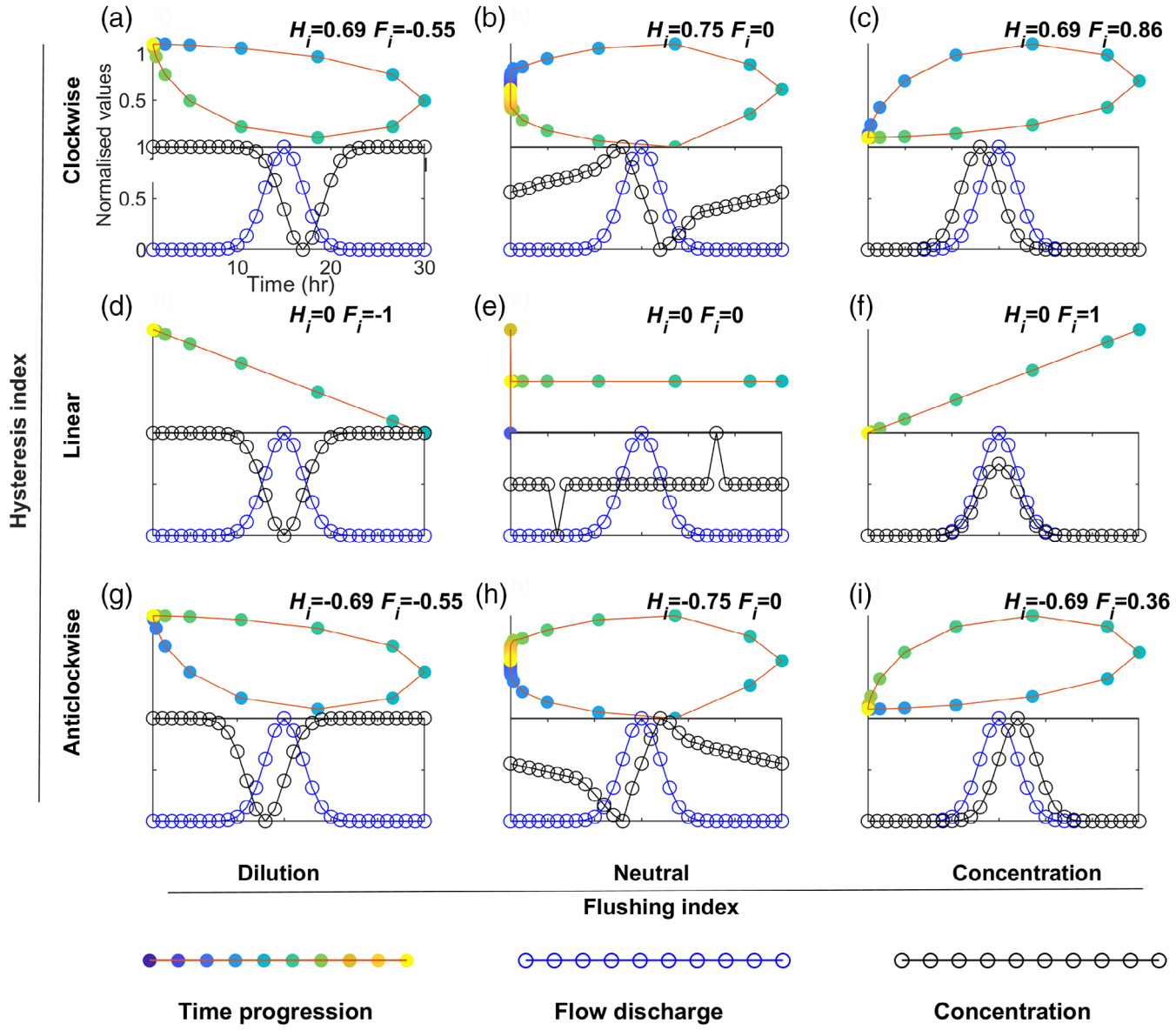

FIGURE 1 Diversity in storm event concentration-discharge (*c-q*) responses expressed as a relation between hysteresis index hi (indicator of the direction of the *c-q* response, clockwise vs. anticlockwise) and flushing index fi (indicator of the impact of storm event on concentrations, concentration vs. dilution). 9 *c-q* types are identified that follow a gradient in hi (anticlockwise hi < –0.1, linear –0.1 > = hi < = 0.1 and clockwise hi > 0.1) and fi (dilution fi < –0.1, neutral –0.1 > = fi < = 0.1 and concentration fi > 0.1). Each graph is labelled as in type a). Top graphs show normalized flow discharge (x-axis) vs. normalized concentrations (y-axis) using colormap from blue to yellow to show time progression of a storm event (in hours). Bottom graphs show normalized flow discharge (blue line) and concentrations (black line) vs. time, corresponding to the top graph

3 | RESULTS

3.1 | Diversity in *c-q* responses

The dataset spans over five hydrological years (2009–2014) with a total of 342 storm events of which 154 had enough hydrochemical data (data completeness >70%) for all tested water quality parameters. The selected storm events covered a range between 2nd-99th flow discharge percentiles with a similar contribution from summer (Jun–Sep, 63 events) and winter storm events (Nov–Feb, 48 events). Storm events varied significantly in terms of duration of the rising (M μ = 6.5 and SD δ = 5.3 hr) and falling limb (μ = 10.3, δ = 8.3 hr), peak flow discharge (μ = 7.2, δ = 5.3 m^3s^{-1}), volume (μ = 258.2, δ = 555.7 m^3), time from previous (μ = 125.8, δ = 203.0 hr), time to the following storm event (μ = 124.5, δ = 277.6 hr) and API_5 (μ = 18, δ = 12 mm; Table S1).

For the selected 154 storm events and nine water quality parameters, hysteresis (H_i) and flushing indices (F_{i_Point} and F_{i_Mean}) were calculated to describe the diversity in storm event *c-q* responses (Table 2). In general, H_i was close to zero for most of the parameters

TABLE 2 Storm *c-q* indices (hysteresis index *Hi* and flushiness index *Fi*). F_{i_Point} is F_i calculated as in Butturini et al., 2008, F_{i_Mean} is F_i calculated for mean concentrations before and during the storm event, F_{i_Trend} is F_{i_Mean} calculated for trend and F_{i_Amp} is F_{i_Mean} calculated for amplitude

	H_i				F_{i_Point}				F_{i_Mean}				F_{i_Trend}				F_{i_Amp}			
Parameter	μ	δ	*S*	*W*	μ	δ	*S*	*W*	μ	δ	*S*	*W*	μ	δ	*S*	*W*	μ	δ	*S*	*W*
TP	0.02	0.34	**−0.13**	**0.14**	0.34	0.38	0.31	0.34	0.29	0.35	0.33	0.23	0.19	0.33	**0.31**	**0.10**	0.17	0.38	0.27	0.14
TRP	−0.03	0.37	**−0.16**	**0.12**	0.22	0.36	0.25	0.10	0.22	0.32	**0.26**	**0.07**	0.17	0.30	**0.27**	**0.04**	0.14	0.40	0.14	0.06
TURB	0.01	0.34	**−0.12**	**0.11**	0.49	0.36	**0.37**	**0.54**	0.40	0.36	**0.29**	**0.44**	0.21	0.37	0.22	0.13	0.16	0.42	0.16	0.09
NO_3-N	0.06	0.44	**−0.04**	**0.24**	−0.01	0.16	**0.02**	**−0.10**	−0.02	0.12	**0.02**	**−0.08**	−0.02	0.18	**0.02**	**−0.12**	0.15	0.31	0.13	0.15
DO	0.00	0.39	**0.12**	**−0.11**	−0.02	0.12	−0.02	−0.03	−0.03	0.10	−0.04	−0.03	−0.05	0.15	−0.04	−0.05	−0.10	0.33	**−0.10**	**0.04**
COND	0.12	0.41	**0.00**	**0.26**	−0.05	0.09	***−0.03***	***−0.07***	−0.03	0.08	−0.02	−0.04	−0.04	0.10	−0.02	−0.04	−0.01	0.35	***−0.11***	***0.06***
RED	−0.12	0.41	**−0.01**	**−0.25**	−0.10	0.40	0.00	−0.01	0.05	0.45	0.01	0.03	−0.01	0.16	0.02	−0.01	−0.03	0.33	0.01	−0.02
pH	0.17	0.37	**0.13**	**0.32**	−0.01	0.02	***0.00***	***−0.01***	−0.01	0.02	***0.00***	***−0.01***	−0.02	0.12	**−0.02**	**−0.03**	−0.05	0.23	−0.05	−0.02
TEMP	0.01	0.43	0.04	−0.03	−0.01	0.07	0.00	0.00	−0.01	0.09	−0.01	0.01	−0.03	0.18	−0.05	0.01	−0.04	0.30	−0.02	−0.06

Note: Pairwise (*S* vs. *W*) Kruskal–Wallis one-way analysis of variance with *p* values at .01 (bold) and .05 (bold italics) significance levels.
Abbreviations: μ, mean value; δ, standard deviation; *S*, summer storms values (June–September); *W*, Winter storms values (November–February).

suggesting a similar contribution from storm events with a positive and negative H_i. The flushing index F_{i_Point} showed a larger variation, with high positive values for TP (μ = 0.34, δ = 0.22), TRP (μ = 0.22, δ = 0.36) and TURB (μ = 0.49, δ = 0.36) indicating a strong concentration response and low, near zero values for the remaining parameters (NO_3-N, DO, COND, RED, pH and TEMP).

From nine possible *c-q* types based on the distribution of H_i and F_i values (Figure 1), the parameters showed a strong preference towards just four types (Table 3): type *b* neutral-clockwise (pH 64.3%, TEMP 41.6%, COND 39.6%), type *c* concentration-clockwise (TP 57.8% and TURB 34.4%), type *h* neutral anticlockwise (RED 62.3%, NO_3-N 50.6%, DO 41.6%) and type *i* concentration-anticlockwise (TRP 31.3%; Table 2). From a total of 154 storm events, 151 showed a unique combination of *c-q* types.

There were significant seasonal differences in H_i and F_i for several parameters (Figure 2, Table 2 and Figure S2). Anticlockwise summer (H_i < 0) and clockwise winter (H_i > 0) storm events were typical for TP, TRP, TURB and NO_3-N. Both DO and RED showed an opposing trend (summer clockwise/neutral and winter anticlockwise response) and COND and pH showed a strong preference towards clockwise events with higher H_i for winter storm events. Fewer parameters showed significant seasonal trends in F_i, with a stronger concentration response for TURB and stronger dilution for NO_3-N and COND in winter (Table 2). Summer storm events showed on average (Figure S3) a lower magnitude (Q_{max} *S* 5.2, *W* 12.1 m^3s^{-1} and Q_{vol} *S* 161.3, *W* 440.1 m^3) and a higher air temperature (*S* 16.3, *W* 8.6 °C) compared to winter storm events.

3.2 | Flushing and cycling responses and their controls

To investigate the effect of storm events on hydrological flushing and biogeochemical cycling, we compared normalized values of trend and amplitude for before (BF), during (ST) and after (AF) storm event for all 154 storm events (Figures 3 and 4). There were two significant patterns in trend: a predominant concentration response for TP, TRP and TURB, and a predominant dilution response for DO, COND, RED and pH. There were no significant differences in trend for NO_3-N and TEMP, suggesting a similar contribution of concentration and dilution responses (Figure 3). Nutrients and sediments showed significant patterns in amplitude, with a strong enhancement effect. The parameters of ecological importance (DO, pH, RED, TEMP and COND) showed in general a dampening response during storm events. However, these patterns were statistically significant only for DO (rising limb) and TEMP (both rising and falling limb). The enhancement effect for nutrients and sediments was restricted to the actual storm event, while the dampening effect for DO and pH extended beyond the duration of the storm event.

Several of the parameters showed significant seasonal differences in F_{i_Trend} and F_{i_Amp} (Table 2). Nutrients and sediments showed higher values of F_{i_Trend} and DO and COND showed lower values of F_{i_Amp} during summer storm events. Several potential controls were

TABLE 3 Diversity of storm event *c-q* responses: Percentage contribution of each *c-q* response type (as in Figure 1)

	Contribution of each *c-q* response (%)								
Parameter	***a***	***b***	***c***	***d***	***e***	***f***	***g***	***h***	***i***
TP	4.5	1.9	**57.8**	1.3	2.6	9.1	3.2	2.6	**17.0**
TRP	11.7	7.8	**18.8**	2.6	1.9	14.9	3.2	7.8	**31.3**
TURB	1.3	5.2	**34.4**	0.6	2.6	21.4	0.0	7.8	**26.7**
NO_3-N	13.0	**19.5**	3.2	1.3	3.2	1.3	0.6	**50.6**	7.3
DO	12.3	**21.4**	4.5	2.6	9.7	0.6	4.5	**41.6**	2.8
COND	16.2	**39.6**	0.0	3.9	9.1	0.6	1.3	**27.9**	1.4
RED	1.3	**25.3**	1.3	0.0	5.8	0.0	2.6	**62.3**	1.4
pH	0.0	**64.3**	0.0	0.0	13.0	0.0	0.0	**22.7**	0.0
TEMP	5.2	**41.6**	0.6	1.3	9.1	0.0	2.6	**36.4**	3.2

Note: The highest two contributions per parameter are marked in bold.

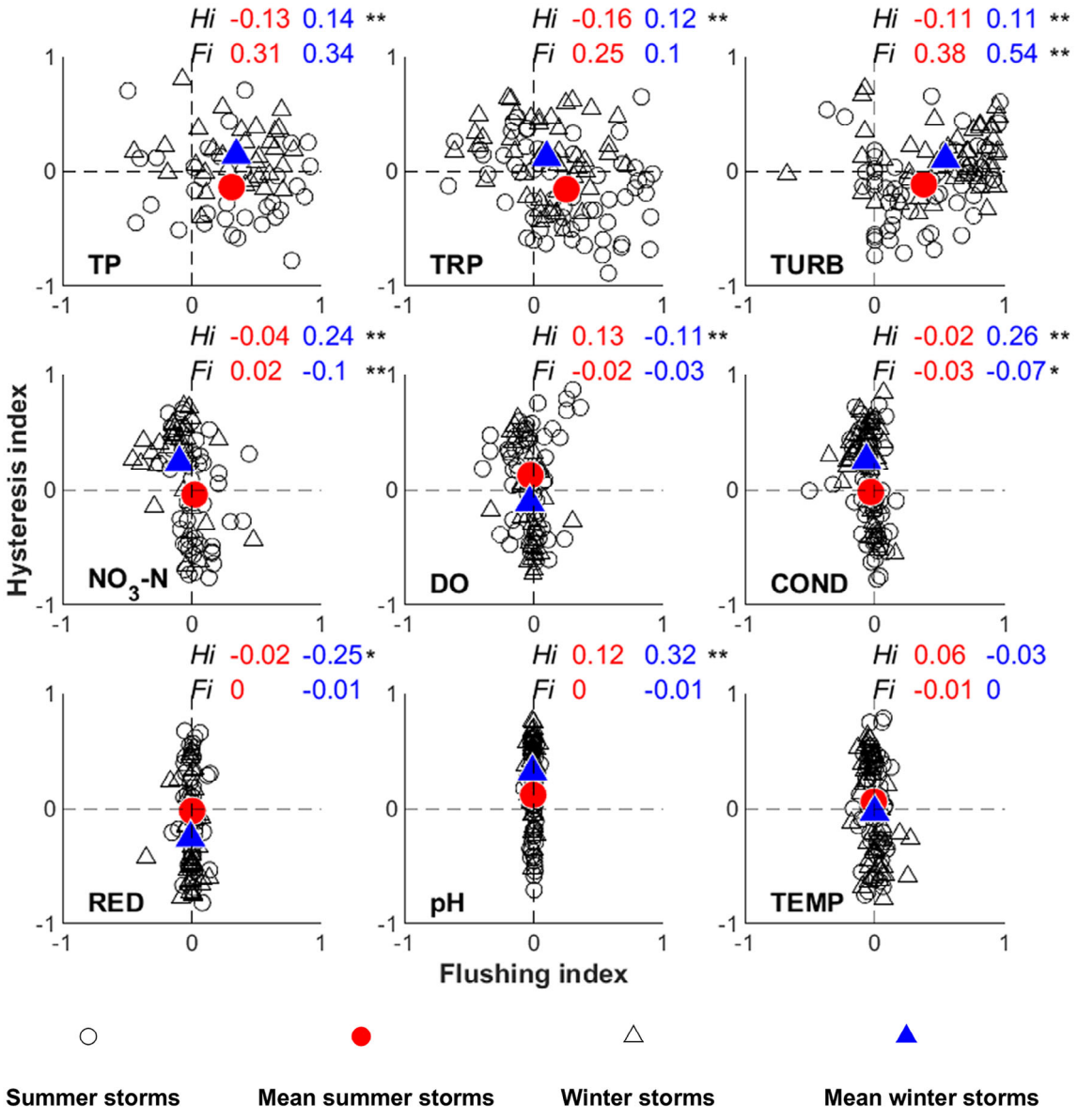

FIGURE 2 Distribution of *c-q* responses for 154 storm events for nine determinands. COND, conductivity; DO, dissolved oxygen; NO_3-N, nitrate nitrogen; pH, TEMP, water temperature; RED, redox potential; TP, total phosphorus; TRP, total reactive phosphorus, TURB, turbidity. Text: Pairwise (hi summer and winter, fi summer and winter) Kruskal–Wallis one-way analysis of variance with *p* values at .01 (**) and .05 (*) significance levels. Summer storm indices in red and winter storm indices in blue

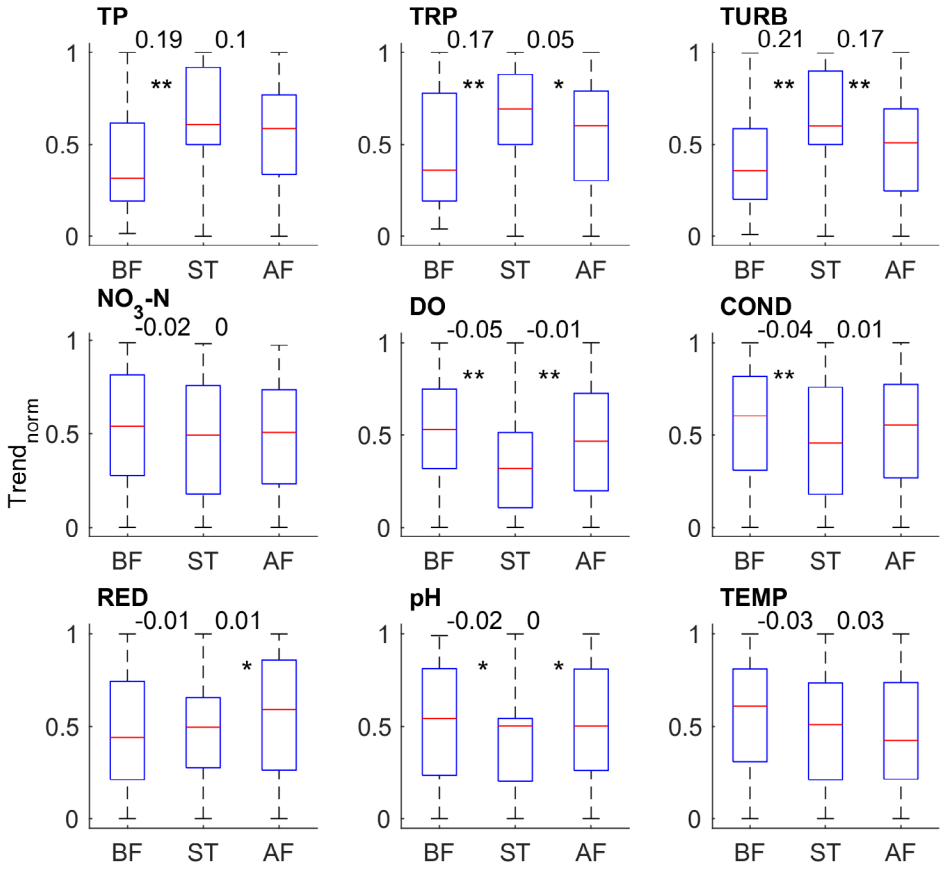

FIGURE 3 Trends for before, during and after storm event (BF, ST, AF), normalized for individual storm events. Pairwise (BF-ST and ST-AF) Kruskal–Wallis one-way analysis of variance with *p* values at .01 (**) and .05 (*) significance levels. Each boxplot is based on data from 154 storm events and shows median value in red, 25th and 75th percentiles as a blue box and the black whiskers extend to the most extreme data points that are not outliers. Fi indices calculated for the rising and falling limb are given as numbers above the plots

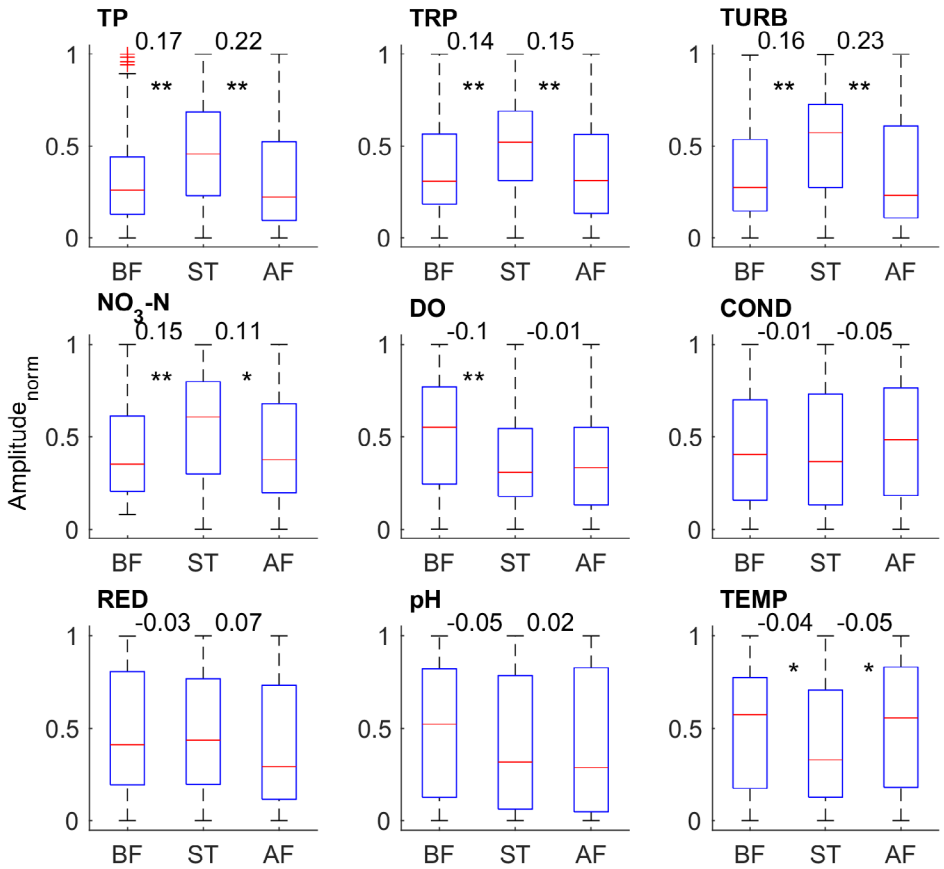

FIGURE 4 Amplitudes for before, during and after storm event (BF, ST, AF), normalized for individual storm events. Pairwise (BF-ST and ST-AF) Kruskal–Wallis one-way analysis of variance with *p* values at .01 (**) and .05 (*) significance levels. Each boxplot is based on data from 154 storm events and shows median value in red, 25th and 75th percentiles as a blue box and the black whiskers extend to the most extreme data points that are not outliers. Fi indices calculated for the rising and falling limb are given as numbers above the plots

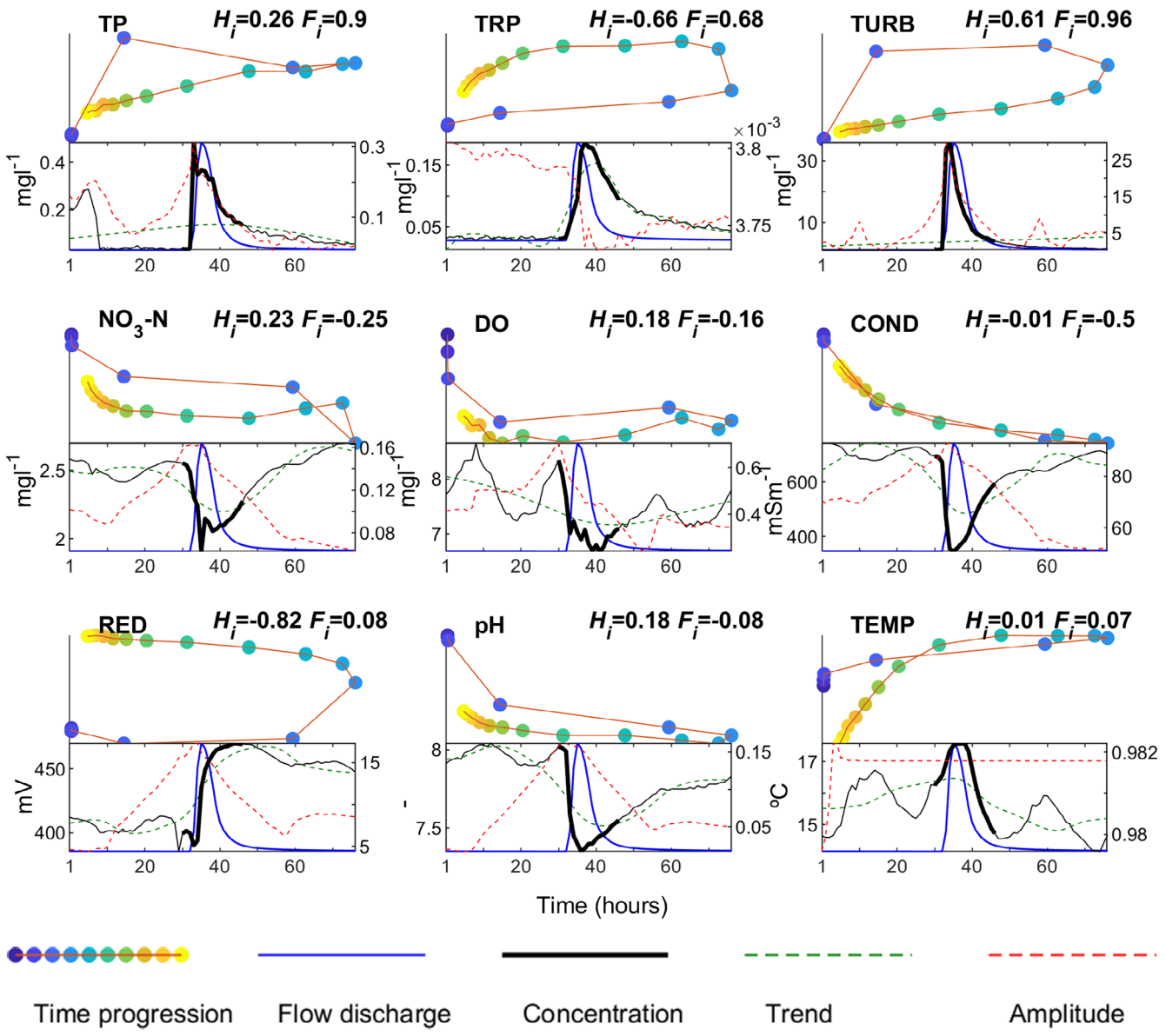

FIGURE 5 Hydrochemical dynamics before, during and after a high-magnitude storm event 93 (28–29 June 2012, Q_{max} = 155 m^3s^{-1}, Q_{vol} = 3565 m^3, time from previous storm event 122 hr). Top graphs show normalized flow discharge (x-axis) vs. normalized concentrations (y-axis) using colormap from blue to yellow to show time progression of a storm event (in hours). Bottom graphs show normalized flow discharge (blue line), concentrations (black line), trend (green dashed line) and amplitude (red dashed line) vs. time (before, during and after the storm event). The left-hand y-axis refers to concentrations and trend and the right-hand side y-axis refers to amplitude, all in the same units. Storm event concentrations during the storm event (corresponding to the top graph) are shown as a wide black line

evaluated (Table S4): a concentration response in trend was typical for storm events with a longer rising limb, longer time from previous storm event, lower API_5 and higher air temperature for TP and TRP. For NO_3-N, DO, COND, RED, pH, the opposite was true. We observed a general concentration effect for storm events with a shorter rising limb and lower Q_{max}. Enhanced diel cycles were observed for lower Q_{max} and longer time from previous storm event for nutrients and for higher Q_{max} and shorter time from previous storm event for COND and DO. We further investigated the impact of Q_{max} on the observed patterns by separating patterns in trend and amplitude for high- and low-magnitude storm events (Figure S6).

The *c-q* responses during high- (Figure 5) and low-magnitude (Figure 6) storm events were generally mirrored: predominantly clockwise responses during the high-magnitude event and predominantly anticlockwise responses during the low-magnitude storm event. During both storms, nutrients and sediments behaved similarly with a predominant concentration response for TP, TRP and TURB and a dilution response for NO_3-N. The other parameters behaved differently: DO, COND and pH showed dilution during the high-magnitude event and concentration during the low-magnitude event and RED and TEMP showed concentration during the high-magnitude event and dilution during the low-magnitude event.

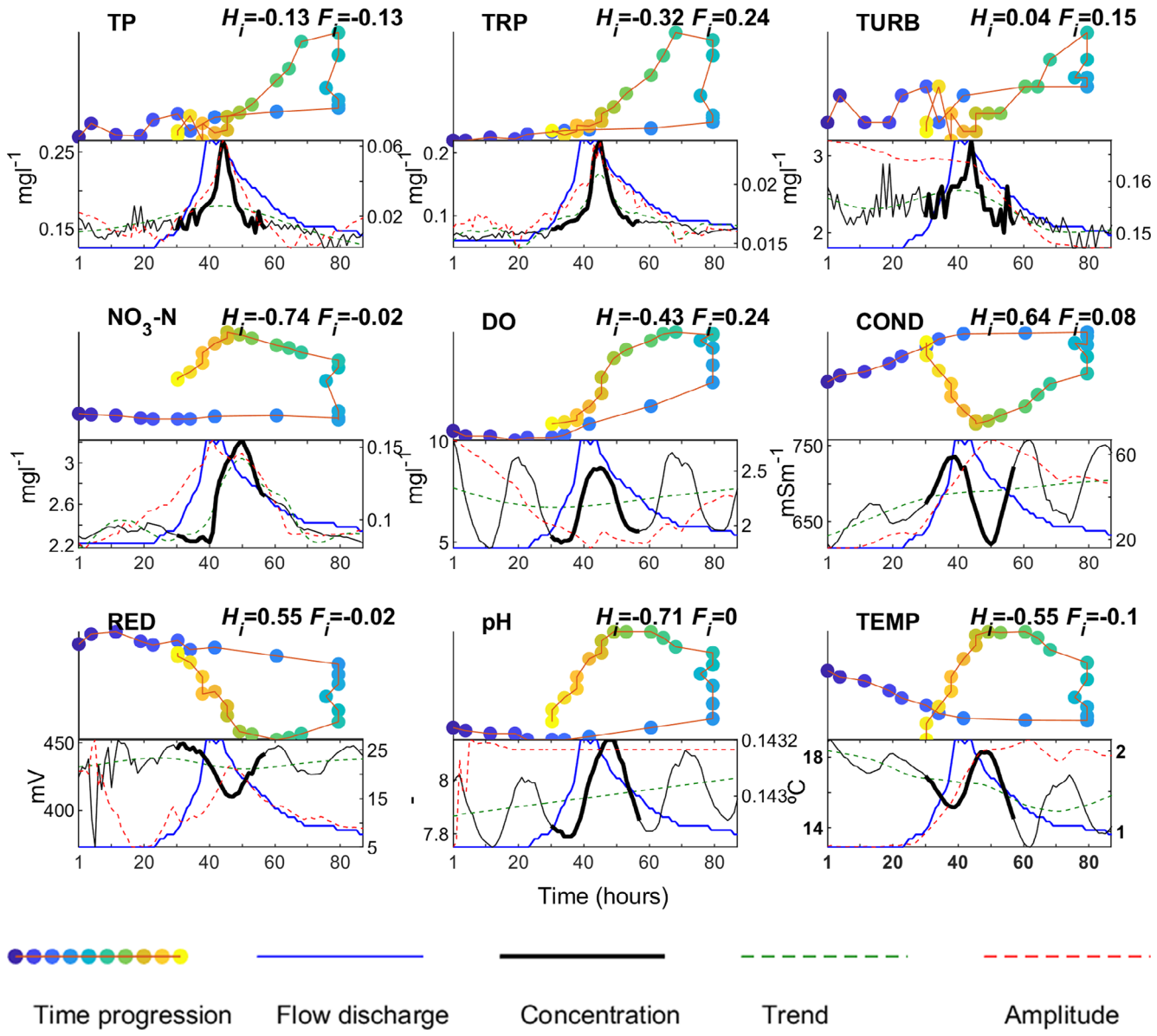

FIGURE 6 Hydrochemical dynamics before, during and after a high-magnitude storm event 140 (4–6 July 2014, Q_{max} = 0.4 m^3s^{-1}, Q_{vol} = 32 m^3, time from previous storm event 503 hr). Top graphs show normalized flow discharge (x-axis) vs. normalized concentrations (y-axis) using colormap from blue to yellow to show time progression of a storm event (in hours). Bottom graphs show normalized flow discharge (blue line), concentrations (black line), trend (green dashed line) and amplitude (red dashed line) vs. time (before, during and after the storm event). The left-hand y-axis refers to concentrations and trend and the right-hand side y-axis refers to amplitude, all in the same units. Storm event concentrations during the storm event (corresponding to the top graph) are shown as a wide black line

Separation of the concentration time series into trend and diel signal, allowed distinguishing between the flushing and cycling responses during both storm events. For most parameters F_{i_Amp} was positive indicating enhancement of the diel cycle with exception of TRP during the high-magnitude storm event, TURB during the low-magnitude storm event and DO which consistently showed a dampening response. Several parameters showed opposing effects in trend and amplitude: trend dilution and amplitude enhancement for NO_3-N, DO, COND, pH, RED, TEMP and trend concentration and amplitude dampening during the low-magnitude storm event for TURB.

3.3 | Is the flushing index a correct representation of concentration changes during storm events?

We found that NO_3-N, DO, COND, RED, pH and TEMP showed stability in the flushing indices with near zero values of F_i for different seasons and storm events, indicating that concentrations at the beginning of the storm event (C_b) were similar to concentrations at the peak flow discharge (C_s). As these parameters exhibit strong diel cycling (Table S2), we examined how the presence of a diurnal cycle can affect both H_i and F_i (Figure S4). Depending on the phase of the diel cycle in relation to the storm event, both parameters can cover a full

range of values from strong anticlockwise (H_i = −0.58) to clockwise response (H_i = 0.58) and from strong dilution (F_i = −1.0) to strong concentration response (F_i = 1.0).

We compared two flushing indices: F_{i_point} calculated from a single concentration at the beginning of the storm event and at the peak flow discharge (Butturini et al., 2008) and F_{i_Mean} based on average concentrations before and during the storm event. We found that there was a good agreement between F_{i_Point} and F_{i_Mean} overall (Figure S5) and for the high-magnitude storm events but a poorer agreement for the low-magnitude storm events with noisy data, diel patterns and multiple peaks (Table 2). An example of this effect can be seen for a low-magnitude storm event in Figure 6 and Table S3. The F_{i_Point} provided a false representation of flushing behaviour for NO_3-N, where F_{i_Point} = −0.02 indicated a weak dilution response but it was a clear concentration response, correctly captured by F_{i_Mean} = 0.12 and F_{i_Trend} = 0.12. A similar effect was observed for TP where a delay in concentration peak (H_i = −0.13) resulted in a false classification of the response as dilution (F_{i_Point} = −0.13) with all other parameters suggesting concentration: F_{i_Mean} = 0.15 and F_{i_Trend} = 0.12 (Table S3). The presence of a diel cycle for DO in phase with peak flow, resulted in a high value of F_{i_Point} = 0.24, suggesting a concentration response. However, all other parameters were negative (F_{i_Mean} = −0.03 and F_{i_Trend} = −0.03) indicating a weak dilution and dampening response.

4 | DISCUSSION

4.1 | Diversity in concentration-discharge responses

Our results showed that (1) there was a large variation in storm event *c-q* responses as almost all storm events revealed a unique pattern of *c-q* types based on the H_i hysteresis index and F_i flushing index, (2) each parameter had a tendency towards just one or two *c-q* types that explain the majority of the observed variance, from 50%–60% for TRP, TURB and DO to 70%–80% for COND, NO_3-N, TEMP, TP, RED and pH, and (3) these patterns changed on a seasonal basis.

The large variation in the *c-q* responses observed in our study suggests that the pattern of mobilization and delivery along with availability and proximity of the sources in relation to the stream, change from storm event to storm event, similar to other studies investigating storm event hydrochemical patterns (Butturini et al., 2008; Minaudo et al., 2019). Hydrochemical indices are widely used to describe solute or particulate behaviour in terms of the timing of the concentration change in relation to flow discharge (H_i) and the magnitude of this change (F_i) (Bieroza & Heathwaite, 2015; Blaen et al., 2017; Butturini et al., 2008; Lloyd et al., 2016b). This information can be then used to explain the dominant sources of solutes and particulates along with their mobilization and delivery pathways (H_i) and the relationship between solute or particulate concentrations in different compartments of the hydrograph (F_i). Positive values of H_i (clockwise responses) indicate mobilization of a readily available source of solutes or particulates (e.g., erosion of river bed sediments) and/or their delivery along relatively short pathways (e.g. from the hyporheic and riparian zones) (Bernhardt et al., 2017). Negative values of H_i (anticlockwise responses) indicate a distant source, delayed mobilization and/or longer delivery pathways (e.g., from isolated locations in the catchment or along subsurface flow pathways) (Bieroza & Heathwaite, 2015). The F_i defines a concentration change between pre- and during the storm event, and therefore reflects differences in concentrations between old, pre-event water and new storm event water. Positive values of F_i (concentration responses) indicate that storm water has higher concentrations or becomes enriched in concentrations of a given solute or particulate by flushing surface or shallow subsurface flow pathways near the stream for example, in the riparian zone (Minaudo et al., 2019). Negative values of F_i (dilution responses) indicate that storm water dilutes higher concentrations of the pre-event water for example, derived from groundwater flows, hyporheic zone or deeper subsurface flow pathways.

The relative timing of solute/particulate mobilization in relation to flow (H_i) in our study changed on a seasonal basis. Nutrients and sediments (TP, TRP, NO_3-N and TURB) were mobilized from the readily available near stream sources and shorter delivery pathways during winter (clockwise responses) and from distant, subsurface sources and pathways during summer (anticlockwise responses). Dissolved oxygen and RED exhibited the opposite pattern (clockwise in summer and anticlockwise in winter) with COND and pH only showing the clockwise responses but weaker in summer and stronger in winter. These seasonal differences in mobilization were likely driven by changes in the storm event magnitude (predominantly low-magnitude in summer and high-magnitude storm events in winter) and air temperature (higher temperatures in summer and lower in winter). Similar results, that succession of linear and nonlinear (clockwise and anti-clockwise) nutrients and sediments *c-q* responses was driven by the magnitude of storm events were found in other studies (Butturini et al., 2008; Lloyd et al., 2016b).

Fewer statistically significant seasonal patterns were observed in the flushing responses, which may indicate variation in source/delivery patterns from storm to storm as the controlling factor for the flushing behaviour for TP, TRP and TURB (concentration) and dilution response for NO_3-N. The strongest concentration response was observed for TURB and TP, indicating that a large portion of the phosphorus pool is driven by sediment transport (Lloyd et al., 2016b). Total reactive P showed a mixed dilution-concentration pattern that may indicate a switch between delivery from shallow pathways (as TURB and TP) and dilution of point sources (e.g., sewerage systems) or P-rich shallow subsurface pathways. As both point and groundwater sources should become more pronounced during summer when low flows tend to dominate (Charlton et al., 2018), the apparent lack of seasonal differences in TRP flushing suggests that TRP transport is driven by storm to storm retention and flushing mechanisms. For the remaining parameters (NO_3-N, DO, COND, RED, pH and TEMP), there was a better correlation with the magnitude of the storm event than with seasonality.

TABLE 4 Conceptual model of flushing and cycling behaviour during high and low-magnitude storm events

		High-magnitude storm events			Low-magnitude storm events		
		Mobilization	Flushing	Cycling	Mobilization	Flushing	Cycling
Parameter		H_i	F_{i_Trend}	F_{i_Amp}	H_i	F_{i_Trend}	F_{i_Amp}
Flushing dominated	TP	Clockwise	Concentration	Enhanced	Anti-clockwise	Concentration	Enhanced
	TRP						
	TURB						
Mixed flushing-cycling	NO_3-N	Clockwise	Dilution	Enhanced	Anti-clockwise	Concentration	Enhanced
	COND						Dampened
	pH			Dampened			
Cycling dominated	DO	Anti-clockwise	Dilution	Dampened	Clockwise	Dilution	Dampened
	RED		—	—			Enhanced
	TEMP	—	—	Dampened	—		Dampened

Note: A dash (—) signifies no clear pattern.
Abbreviations: COND, specific conductivity; NO_3-N, Nitrate nitrogen; pH, DO, dissolved oxygen; RED, redox potential; TEMP, water temperature; TP, total phosphorus; TRP, total reactive phosphorus; TURB, turbidity.

4.2 | The interplay between hydrological flushing and biogeochemical cycling

To date, most studies have focused on either flushing and storm events (see e.g., (Bieroza & Heathwaite, 2015; Blaen et al., 2017; Boyer et al., 1997) or cycling and diel patterns, see for example (Burns et al., 2016; Ensign & Doyle, 2006). Our approach allowed us to conceptualise the dual flushing-cycling behaviour in relation to the magnitude of the storm events (Table 4) that we determined to be the critical factor controlling the *c-q* responses. Three groups of parameters were identified corresponding to flushing dominated (TP, TRP and TURB), cycling dominated (DO, RED and TEMP) and parameters exhibiting a mixed flushing-cycling behaviour (NO_3-N, COND and pH). In general, the magnitude of a storm event appeared to control the pattern of mobilization, with high-magnitude storm events driving rapid mobilization (clockwise response), and low-magnitude storm events driving delayed mobilization (anticlockwise response) for both flushing and mixed type parameters. The opposite pattern was displayed by the cycling dominated parameters. Both flushing and cycling patterns were stable for the flushing dominated parameters (concentration and enhancement) and cycling dominated parameters (dilution and dampening), regardless of the magnitude of a storm event. The mixed type parameters showed mixed patterns: dilution and enhancement during high-magnitude storm events and concentration and dampening during low-magnitude storm events.

The predominance of a given flushing pattern is likely to be linked to the major source of the chemical. For example, Knapp et al. (2020) distinguished different *c-q* behaviour types for solutes of different origin: predominantly concentration behaviour for soil-sourced solutes, predominantly dilution behaviour for groundwater-sourced solutes and a mixed behaviour for solutes derived from different sources. The chemical origin can also play a role in the predominant direction of the *c-q* relationship on an event-scale. For example, Rose et al. (2018) showed that geogenic solutes (calcium or nitrate) show predominantly a clockwise response, while biologically associated solutes show predominantly an anticlockwise response. These findings corroborate to some extent our results that low-magnitude storm events with more pronounced biogeochemical cycling exhibit mostly anticlockwise responses, while high-magnitude storm events with more pronounced hydrological flushing show mostly clockwise responses. However, this pattern was not supported for two cycling dominated parameters DO and RED, which suggests that *c-q* relationships for different catchments, storm events and parameters can be highly variable.

Storm events are periods of rapid changes in physical, chemical and biological variables in riverine systems, with the changes in shear stress, nutrient availability, increased turbidity and reduced light penetration being the most critical. This disturbance can either enhance or dampen the biogeochemical processes and the amplitude of diel cycles (Woodward et al., 2016) with a relative balance of flushing and cycling for low-magnitude storms and increased flushing over cycling for high-magnitude storm events (Raymond et al., 2016; Wollheim et al., 2018). High-magnitude storm events often involve stream bed erosion that leads to scouring or burial of the biomass of autotrophic and heterotrophic communities resulting in diminished (Bernhardt et al., 2018) or completely suppressed (Burns et al., 2016) diel cycles. This storm-driven disturbance dampens the biological activity until the communities redevelop and re-establish the diel cycles (Burns et al., 2019). On the other hand, low-magnitude storm events tend to drive only minor increases in turbidity that reduce light availability, which can slightly dampen or have no visible effect on the presence of the diel cycle. Our results showed that diel cycles are, to a large extent, preserved during low-magnitude events, and are rapidly (<24 hr) re-established following high-magnitude storm events. This could indicate a potential balance between cycling and flushing during low-magnitude storm events and a dominance of flushing (supply) over cycling (demand) during high-magnitude storm events, in line with the River Network Saturation concept (Wollheim et al., 2018). The parameters with predominant cycling behaviour (DO, pH and

TEMP) showed consistently reduced amplitudes of diel cycles suggesting that the occurrence of the disturbance rather than its magnitude was a controlling factor. For the low-magnitude summer storm events specifically, their increased occurrence was shown to increase delivery of organic matter and benthic respiration resulting in reduced concentrations and the amplitude of diel cycles (Hutchins et al., 2020). We observed enhanced rather than reduced cycling during high-magnitude storm events for some parameters in our study (COND, NO_3-N and DO). This behaviour may be linked to flushing of hyporheic flow pathways and increased efficiency of aerobic respiration and denitrification that is not observed during low-magnitude storm events (Trauth & Fleckenstein, 2017).

4.3 | Advances in understanding hydrochemical processes in-stream systems

The full potential of the new wave of high-frequency measurements and its impact on advancing stream hydrochemistry and ecology (Kirchner et al., 2004) is only just being realised (Benettin & van Breukelen, 2017; Rode, Wade, et al., 2016). Our ability to detect significant patterns in the *c*-*q* data and to conceptualise this behaviour improves with the increasing availability of long-term high-quality and high-frequency datasets, where the challenges with water quality sample degradation over time have been overcome. Improved conceptual models of stream functioning are critical to our understanding of the current and future impacts of multiple stressors on stream ecosystems (Birk et al., 2020). Regional (Ockenden et al., 2017) and global (Seneviratne et al., 2012) hydroclimatic simulations indicate that the frequency of extreme hydrological events is rising, including increased storm and drought occurrence. Such events are predicted to increase in frequency, intensity and duration with knock-on consequences for freshwater ecology (Ouellet et al., 2020; Woodward et al., 2016) including under baseflow conditions (Arnell, 2004) and especially for nutrients in groundwater-fed river systems, for example (Trauth & Fleckenstein, 2017). Long-term high-frequency datasets can provide examples of system behaviour in response to these extreme hydrological events and therefore yield information on their potential sensitivity to global change. The hydrochemical indices can serve as an indicator of such change shifts and be used as functional measures for assessing freshwater quality. For catchments, where relationships between storm event magnitude and hydrochemical indices can be established, it is possible to provide information on the dominant sources, mobilization and delivery patterns. Inference can be made of how disturbance and recovery times impact on stream biota if changes before and after the storm event are considered. Where systemic changes to this pattern are observed, they may be indicative of a stream ecosystem change with respect to the potential for the provision of critical ecosystem services including nutrient retention (Bunn, 2016; IPBES, 2019; Vorosmarty et al., 2018). The hydrochemical indices can be applied as diagnostic tools in catchment management for comparing behaviour and grading sensitivity to disturbance of different stream ecosystems, particularly if subjected to multiple stressors (Birk et al., 2020). The ratio of flushing indices for trend (a proxy for flushing) and amplitude (a proxy for cycling) could be calculated to evaluate a relative importance of hydrological vs. biogeochemical controls. Such an approach could help to test conceptual frameworks of River Network Saturation concept (Wollheim et al., 2018) and pulse-shunt concept (Raymond et al., 2016) over a range of hydrological conditions and stream networks.

We recommend the calculation of flushing indices to provide insight into average concentration characteristics for periods of interest (e.g., before, during and after the storm event) because reliance on point values as suggested by (Butturini et al., 2008) may lead to a flawed representation of the *c*-*q* relationship. Testing flushing indices (F_{i_Mean}) for both the rising and the falling limbs of a storm event, and extending this analysis to periods between the storm events, can yield additional insights regarding the impact of storm events on biogeochemical processes but also impact of biogeochemical retention of solutes and particulates on flushing behaviour. For some parameters in our study (DO and pH) the dampening effect of a storm event on the amplitude of the diurnal cycle lasted well beyond the 30 hrs used to define the period after the storm event. These changes in amplitude might be subtle but may indicate long-lasting disturbance effects on stream ecology (Hutchins et al., 2020).

4.4 | Potential limitations

Our approach applied to decompose the water quality signal into underlying trend and amplitude of diel cycle requires further testing. While the DHR decomposition method is widely accepted (Halliday et al., 2012; Young et al., 1999), it may be less suited to model *c*-*q* dynamics for shorter storm events (<24 hrs). We sought to avoid these issues by modelling a longer time series including the time before, during and after individual storm events (>60 hrs). Further, the risk that observed patterns are model artefacts requires evaluation, particularly whether the trend and cyclical components are independent or there is a spectral overlap and thus a correlation between concentration/enhancement and dilution/dampening patterns. Our results indicate, however, that there was a large variation in flushing-cycling responses including also concentration/dampening and dilution/enhancement patterns. Another potential limitation is the possibility of hydrological and biogeochemical processes both contributing to trend and amplitude of the cyclical component. To test this, an independent way of decomposing signals into hydrological and biogeochemical components is needed, for example, by the use of hydrochemical models, data mining approaches and in situ estimation of the rates of biogeochemical processes (Aubert et al., 2016). This alternative approach is particularly needed when no apparent diel cycle can be detected in the water quality time series and the signal decomposition used in our study cannot be justified. Limiting nutrients often do not exhibit diel cycles due to rapid uptake (Hensley & Cohen, 2016); however, in highly polluted agricultural streams a N and P co-limitation is common along with limitation from other factors e.g. light availability (Jarvie et al., 2018). A lack of diel cycle can also

result from different biogeochemical processes producing asynchronous diel cycles (Nimick et al., 2011).

As our results show, both H_i and F_i indices are potentially highly sensitive to the presence of diel cycles in modelled time series. As the period of diel cycle versus storm event should be random (Figure S1), one can expect a large variation in both hysteresis and flushing indices. Indeed, the hysteresis index H_i showed a large variation in clockwise and anticlockwise responses. However, since similar patterns in H_i were observed for flushing, mixed type and cycling dominated parameters in response to common drivers (magnitude of a storm event and seasonality), we conclude that the H_i values presented in our study were not biased. Unlike the H_i, the flushing index F_i showed a very narrow range for the mixed type and cycling dominated parameters as most of the responses were classified as flushing neutral ($-0.1 < F_i < 0.1$). This flushing type is likely related to a chemostatic response to flow for several parameters in our study (Godsey et al., 2019). The concentrations of NO_3-N, COND, pH and RED can be buffered (Bieroza et al., 2014) by the presence of an abundant source of solute from the Penrith Sandstone aquifer (Wang & Burke, 2017). The parameters controlling stream metabolism (DO and TEMP) are dominated by the biogeochemical cycling and therefore potentially less responsive to hydrological flushing. These results suggest that F_i is potentially better suited to representing typically flushing parameters like TP, TRP and TURB with highly episodic response to flow due to anthropogenic pollution (Basu et al., 2011; Bieroza et al., 2014). Novel hydrochemical indices are needed to capture the flushing dynamics of parameters showing a chemostatic behaviour.

5 | CONCLUSIONS

As the frequency of extreme hydrological events is rising, presenting major challenges for the future of freshwater ecosystems (Bunn, 2016), understanding the interplay between the hydrological flushing and biogeochemical cycling is of critical importance (Wollheim et al., 2018). Combining hydrochemical fingerprints, as undertaken in our study, adds value to our understanding of the drivers of freshwater quality and their potential to impact stream ecology. As coined by (Rode, Wade, et al., 2016), we are riding the high-frequency data wave where advances in in situ monitoring enable insights that were not previously observable; this opportunity is akin to the growth in understanding observed in, for example, eDNA in freshwater environments (Seymour, 2019). Freshwater ecosystems underpin human survival regarding water security yet the biodiversity on which their functioning depends remains threatened worldwide despite efforts during the decade of 'Water for Life' (Dudgeon et al., 2006); we are now looking at emergency recovery plans (Tickner et al., 2020). Our capacity to describe environmental impacts (problem identification) and understanding mechanisms, as this paper shows, remains strong. The challenge is applying this understanding towards preventing impacts through predictive science and appropriate regulatory frameworks to deliver sustainable outcomes. To address this research and science-application gap, we suggest piloting hydrochemical indices as metrics that capture key parts of the biogeochemical functioning of stream ecosystems. Their use enables analysis of contemporaneous hydrological flushing (controlled by catchment properties) and biogeochemical cycling (controlled by stream ecosystem properties). Our results show that despite large storm to storm diversity in hydrochemical responses, storm event magnitude and timing have a critical role in controlling the type of mobilization, flushing and cycling behaviour. Understanding of this interplay can help to maximise the provision of stream ecosystem services, which becomes urgently needed to mitigate the negative impacts of global change.

ACKNOWLEDGEMENTS

The authors would like to thank Neil Mullinger (now at CEH Edinburgh) and Paddy Keenan (now at CEH Lancaster) for their help with setting up and managing the in situ monitoring station and data collection, Fiona Smith (Lancaster University) for her operational support and text edits, Włodek Tych (Lancaster University) for his help with the DHR modelling. The project was funded by the Natural Environment Research Council (NE/G001707/1) awarded to A. L. H. M. B. acknowledges funding from the Swedish Research Council FORMAS grant 2018–00890 and the Swedish Farmer's Foundation for Agricultural Research grant O-16-23-640. ALH was principal investigator on the NERC research grant that underpins this analysis. MB undertook the data collection and primary analysis. A. L. H. and M. B. jointly wrote the research paper. M. B. would like to dedicate this paper to the memory of her beloved mother Wiesława Olenderek-Bieroza.

SUPPORTING INFORMATION

Supporting tables include information on storm events (Table S1), diel cycles (Table S2), flushing and cycling for two storm events of contrasting magnitude (Table S3) and analysis of variance in flushing and cycling parameters (Table S4). Supporting figures include information on difference between H_{i_50} and H_{i_Mean} (Figure S1), seasonal differences in H_i and F_i (Figure S2), storm characteristics (Figure S3), the effect of diel cycle on H_i and F_i (Figure S4), differences between F_{i_Point} and F_{i_Mean} (Figure S5) and differences in trend and amplitude (Figure S6).

DATA AVAILABILITY STATEMENT

The data that support the findings of this study are available from the corresponding author upon reasonable request.

ORCID

Ann Louise Heathwaite https://orcid.org/0000-0001-8791-0039
Magdalena Bieroza https://orcid.org/0000-0002-3520-4375

REFERENCES

Abbott, B. W., Gruau, G., Zarnetske, J. P., Moatar, F., Barbe, L., Thomas, Z., … Pinay, G. (2018). Unexpected spatial stability of water chemistry in headwater stream networks. *Ecology Letters*, *21*(2), 296–308. http://dx.doi.org/10.1111/ele.12897.

Ameli, A. A., Beven, K., Erlandsson, M., Creed, I. F., McDonnell, J. J., & Bishop, K. (2017). Primary weathering rates, water transit times, and

concentration-discharge relations: A theoretical analysis for the critical zone. *Water Resources Research*, *53*, 942–960. https://doi.org/10.1002/2016wr019448

Arnell, N. W. (2004). Climate-change impacts on river flows in Britain: The Ukcipo2 scenarios. *Water and Environment Journal*, *18*(2), 112–117. https://doi.org/10.1111/j.1747-6593.2004.tb00507.x

Aubert, A. H., Thrun, M. C., Breuer, L., & Ultsch, A. (2016). Knowledge discovery from high-frequency stream nitrate concentrations: Hydrology and biology contributions. *Scientific Reports*, *6*, 31536. https://doi.org/10.1038/srep31536

Banwart, S. (2011). Save our soils. *Nature*, *474*(7350), 151–152. https://doi.org/10.1038/474151a

Basu, N. B., Thompson, S. E., & Rao, P. S. C. (2011). Hydrologic and biogeochemical functioning of intensively managed catchments: A synthesis of top-down analyses. *Water Resources Research*, *47*(10), 1–12. https://doi.org/10.1029/2011wr010800

Beerling, D. J., Kantzas, E. P., Lomas, M. R., Wade, P., Eufrasio, R. M., Renforth, P., … Banwart, S. A. (2020). Potential for large-scale CO2 removal via enhanced rock weathering with croplands. *Nature*, *583*(7815), 242–248. http://dx.doi.org/10.1038/s41586-020-2448-9.

Benettin, P., & van Breukelen, B. M. (2017). Decomposing the bulk electrical conductivity of streamflow to recover individual solute concentrations at high frequency. *Environmental Science & Technology Letters*, *4*(12), 518–522. https://doi.org/10.1021/acs.estlett.7b00472

Bernhardt, E. S., Blaszczak, J. R., Ficken, C. D., Fork, M. L., Kaiser, K. E., & Seybold, E. C. (2017). Control points in ecosystems: Moving beyond the hot spot hot moment concept. *Ecosystems*, *20*(4), 665–682. https://doi.org/10.1007/s10021-016-0103-y

Bernhardt, E. S., Heffernan, J. B., Grimm, N. B., Stanley, E. H., Harvey, J. W., Arroita, M., … Yackulic, C. B. (2018). The metabolic regimes of flowing waters. *Limnology and Oceanography*, *63*(S1), S99–S118. http://dx.doi.org/10.1002/lno.10726.

Bieroza, M. Z., & Heathwaite, A. L. (2015). Seasonal variation in phosphorus concentration–discharge hysteresis inferred from high-frequency in situ monitoring. *Journal of Hydrology*, *524*, 333–347. https://doi.org/10.1016/j.jhydrol.2015.02.036

Bieroza, M. Z., & Heathwaite, A. L. (2016). Unravelling organic matter and nutrient biogeochemistry in groundwater-fed rivers under baseflow conditions: Uncertainty in in situ high-frequency analysis. *Science of The Total Environment*, *572*, 1520–1533. https://doi.org/10.1016/j.scitotenv.2016.02.046

Bieroza, M. Z., Heathwaite, A. L., Bechmann, M., Kyllmar, K., & Jordan, P. (2018). The concentration-discharge slope as a tool for water quality management. *Science of the Total Environment*, *630*, 738–749. https://doi.org/10.1016/j.scitotenv.2018.02.256

Bieroza, M. Z., Heathwaite, A. L., Mullinger, N. J., & Keenan, P. O. (2014). Understanding nutrient biogeochemistry in agricultural catchments: The challenge of appropriate monitoring frequencies. *Environmental Science. Processes & Impacts*, *16*(7), 1676–1691. https://doi.org/10.1039/c4em00100a

Binley, A., Ullah, S., Heathwaite, A. L., Heppell, C., Byrne, P., Lansdown, K., … Zhang, H. (2013). Revealing the spatial variability of water fluxes at the groundwater-surface water interface. *Water Resources Research*, *49*(7), 3978–3992. http://dx.doi.org/10.1002/wrcr.20214.

Birk, S., Chapman, D., Carvalho, L., Spears, B. M., Andersen, H. E., Argillier, C., … Hering, D. *Nature Ecology & Evolution*, *4*(8), 1060–1068. http://dx.doi.org/10.1038/s41559-020-1216-4.

Blaen, P. J., Khamis, K., Lloyd, C., Comer-Warner, S., Ciocca, F., Thomas, R. M., … Krause, S. (2017). High-frequency monitoring of catchment nutrient exports reveals highly variable storm event responses and dynamic source zone activation. *Journal of Geophysical Research: Biogeosciences*, *122*(9), 2265–2281. http://dx.doi.org/10.1002/2017jg003904.

Botter, M., Li, L., Hartmann, J., Burlando, P., & Fatichi, S. (2020). Depth of solute generation is a dominant control on concentration-discharge relations. *Water Resources Research*, *56*(8). https://doi.org/10.1029/2019wr0266951–18.

Boyer, E. W., Hornberger, G. M., Bencala, K. E., & McKnight, D. M. (1997). Response characteristics of DOC flushing in an alpine catchment. *Hydrological Processes*, *11*(12), 1635–1647. https://doi.org/10.1002/(sici)1099-1085(19971015)11:12<1635::aid-hyp494>3.0.co;2-h

Brocca, L., Melone, F., & Moramarco, T. (2008). On the estimation of antecedent wetness conditions in rainfall–runoff modelling. *Hydrological Processes*, *22*(5), 629–642. https://doi.org/10.1002/hyp.6629

Bunn, S. E. (2016). Grand challenge for the future of freshwater ecosystems. *Frontiers in Environmental Science*, *4*, 1–4. https://doi.org/10.3389/fenvs.2016.00021.

Burns, D. A. (2005). What do hydrologists mean when they use the term flushing? *Hydrological Processes*, *19*(6), 1325–1327. https://doi.org/10.1002/hyp.5860

Burns, D. A., Miller, M. P., Pellerin, B. A., & Capel, P. D. (2016). Patterns of diel variation in nitrate concentrations in the Potomac River. *Freshwater Science*, *35*(4), 1117–1132. https://doi.org/10.1086/688777

Burns, D. A., Pellerin, B. A., Miller, M. P., Capel, P. D., Tesoriero, A. J., & Duncan, J. M. (2019). Monitoring the riverine pulse: Applying high-frequency nitrate data to advance integrative understanding of biogeochemical and hydrological processes. *Wiley Interdisciplinary Reviews: Water*, *6*, e1348. https://doi.org/10.1002/wat2.1348.

Butturini, A., Alvarez, M., Bernal, S., Vazquez, E., & Sabater, F. (2008). Diversity and temporal sequences of forms of DOC and NO3-discharge responses in an intermittent stream: Predictable or random succession? *Journal of Geophysical Research*, *113*(G3). https://doi.org/10.1029/2008jg0007211–10.

Charlton, M. B., Bowes, M. J., Hutchins, M. G., Orr, H. G., Soley, R., & Davison, P. (2018). Mapping eutrophication risk from climate change: Future phosphorus concentrations in English rivers. *Science of the Total Environment*, *613-614*, 1510–1526. https://doi.org/10.1016/j.scitotenv.2017.07.218

Creed, I. F., McKnight, D. M., Pellerin, B. A., Green, M. B., Bergamaschi, B. A., Aiken, G. R., … Smith, R. (2015). The river as a chemostat: fresh perspectives on dissolved organic matter flowing down the river continuum. *Canadian Journal of Fisheries and Aquatic Sciences*, *72*(8), 1272–1285. http://dx.doi.org/10.1139/cjfas-2014-0400.

Dudgeon, D., Arthington, A. H., Gessner, M. O., Kawabata, Z., Knowler, D. J., Leveque, C., … Sullivan, C. A. (2006). Freshwater biodiversity: importance, threats, status and conservation challenges. *Biological Reviews*, *81*(02), 163http://dx.doi.org/10.1017/s1464793105006950.

Dupas, R., Jomaa, S., Musolff, A., Borchardt, D., & Rode, M. (2016). Disentangling the influence of hydroclimatic patterns and agricultural management on river nitrate dynamics from sub-hourly to decadal time scales. *Science of the Total Environment*, *571*, 791–800. https://doi.org/10.1016/j.scitotenv.2016.07.053

Ensign, S. H., & Doyle, M. W. (2006). Nutrient spiraling in streams and river networks. *Journal of Geophysical Research: Biogeosciences*, *111*(G4), 1–13. https://doi.org/10.1029/2005jg000114.

Godsey, S. E., Hartmann, J., & Kirchner, J. W. (2019). Catchment chemostasis revisited: Water quality responds differently to variations in weather and climate. *Hydrological Processes*, *33*(24), 3056–3069. https://doi.org/10.1002/hyp.13554

Godsey, S. E., Kirchner, J. W., & Clow, D. W. (2009). Concentration-discharge relationships reflect chemostatic characteristics of US catchments. *Hydrological Processes*, *23*(13), 1844–1864. https://doi.org/10.1002/hyp.7315

Halliday, S. J., Wade, A. J., Skeffington, R. A., Neal, C., Reynolds, B., Rowland, P., … Norris, D. (2012). An analysis of long-term trends, seasonality and short-term dynamics in water quality data from Plynlimon, Wales. *Science of The Total Environment*, *434*, 186–200. http://dx.doi.org/10.1016/j.scitotenv.2011.10.052.

Heathwaite, A. L. (2010). Multiple stressors on water availability at global to catchment scales: Understanding human impact on nutrient cycles

to protect water quality and water availability in the long term. *Freshwater Biology*, *55*, 241–257. https://doi.org/10.1111/j.1365-2427.2009.02368.x

Hensley, R. T., & Cohen, M. J. (2016). On the emergence of diel solute signals in flowing waters. *Water Resources Research*, *52*(2), 759–772. https://doi.org/10.1002/2015wr017895

Heppell, C., Louise Heathwaite, A., Binley, A., Byrne, P., Ullah, S., Lansdown, K., … Zhang, H. (2013). Interpreting spatial patterns in redox and coupled water–nitrogen fluxes in the streambed of a gaining river reach. *Biogeochemistry*, *117*(2–3), 491–509. https://doi.org/10.1007/s10533-013-9895-4

Hutchins, M. G., Harding, G., Jarvie, H. P., Marsh, T. J., Bowes, M. J., & Loewenthal, M. (2020). Intense summer floods may induce prolonged increases in benthic respiration rates of more than one year leading to low river dissolved oxygen. *Journal of Hydrology X*, *8*, 100056. https://doi.org/10.1016/j.hydroa.2020.100056

IPBES. (2019). Summary for policymakers of the global assessment report on biodiversity and ecosystem services of the intergovernmental science-policy platform on biodiversity and ecosystem services. Retrieved from Bonn, Germany.

Jarvie, H. P., Smith, D. R., Norton, L. R., Edwards, F. K., Bowes, M. J., King, S. M., … Bachiller-Jareno, N. (2018). Phosphorus and nitrogen limitation and impairment of headwater streams relative to rivers in Great Britain: A national perspective on eutrophication. *Science of The Total Environment*, *621*, 849–862. http://dx.doi.org/10.1016/j.scitotenv.2017.11.128.

Johnes, P., Gooddy, D., Heaton, T., Binley, A., Kennedy, M., Shand, P., & Prior, H. (2020). Determining the impact of riparian wetlands on nutrient cycling, storage and export in permeable agricultural catchments. *Water*, *12*(1), 167. https://doi.org/10.3390/w12010167

Kirchner, J. W., Feng, X., Neal, C., & Robson, A. J. (2004). The fine structure of water-quality dynamics: The(high-frequency) wave of the future. *Hydrological Processes*, *18*(7), 1353–1359. https://doi.org/10.1002/hyp.5537

Knapp, J. L. A., von Freyberg, J., Studer, B., Kiewiet, L., & Kirchner, J. W. (2020). Concentration–discharge relationships vary among hydrological events, reflecting differences in event characteristics. *Hydrology and Earth System Sciences*, *24*(5), 2561–2576. https://doi.org/10.5194/hess-24-2561-2020

Krause, S., Heathwaite, L., Binley, A., & Keenan, P. (2009). Nitrate concentration changes at the groundwater-surface water interface of a small Cumbrian river. *Hydrological Processes*, *23*(15), 2195–2211. https://doi.org/10.1002/hyp.7213

Lansdown, K., Heppell, C. M., Trimmer, M., Binley, A., Heathwaite, A. L., Byrne, P., & Zhang, H. (2015). The interplay between transport and reaction rates as controls on nitrate attenuation in permeable, streambed sediments. *Journal of Geophysical Research: Biogeosciences*, *120*(6), 1093–1109. https://doi.org/10.1002/2014jg002874

Lewandowski, J., Meinikmann, K., & Krause, S. (2020). Groundwater–surface water interactions: Recent advances and interdisciplinary challenges. *Water*, *12*(1), 296. https://doi.org/10.3390/w12010296

Lloyd, C. E., Freer, J. E., Johnes, P. J., & Collins, A. L. (2016a). Technical note: Testing an improved index for analysing storm discharge–concentration hysteresis. *Hydrology and Earth System Sciences*, *20*(2), 625–632. https://doi.org/10.5194/hess-20-625-2016

Lloyd, C. E., Freer, J. E., Johnes, P. J., & Collins, A. L. (2016b). Using hysteresis analysis of high-resolution water quality monitoring data, including uncertainty, to infer controls on nutrient and sediment transfer in catchments. *Science of the Total Environment*, *543*, 388–404. https://doi.org/10.1016/j.scitotenv.2015.11.028

Lynch, L. M., Sutfin, N. A., Fegel, T. S., Boot, C. M., Covino, T. P., & Wallenstein, M. D. (2019). River channel connectivity shifts metabolite composition and dissolved organic matter chemistry. *Nature Communications*, *10*(1), 459. https://doi.org/10.1038/s41467-019-08406-8

MathWorks. (2018). *Matlab version 9.4 R2018b*. The MathWorks Inc.

Minaudo, C., Dupas, R., Gascuel-Odoux, C., Fovet, O., Mellander, P.-E., Jordan, P., … Moatar, F. (2017). Nonlinear empirical modeling to estimate phosphorus exports using continuous records of turbidity and discharge. *Water Resources Research*, *53*(9), 7590–7606. http://dx.doi.org/10.1002/2017wr020590.

Minaudo, C., Dupas, R., Gascuel-Odoux, C., Roubeix, V., Danis, P.-A., & Moatar, F. (2019). Seasonal and event-based concentration-discharge relationships to identify catchment controls on nutrient export regimes. *Advances in Water Resources*, *131*, 103379. https://doi.org/10.1016/j.advwatres.2019.103379

Moatar, F., Abbott, B. W., Minaudo, C., Curie, F., & Pinay, G. (2017). Elemental properties, hydrology, and biology interact to shape concentration-discharge curves for carbon, nutrients, sediment, and major ions. *Water Resources Research*, *53*, 1270–1287. https://doi.org/10.1002/2016wr019635

Nimick, D. A., Gammons, C. H., & Parker, S. R. (2011). Diel biogeochemical processes and their effect on the aqueous chemistry of streams: A review. *Chemical Geology*, *283*(1–2), 3–17. https://doi.org/10.1016/j.chemgeo.2010.08.017

Ockenden, M. C., Deasy, C. E., Benskin, C. M., Beven, K. J., Burke, S., Collins, A. L., … Haygarth, P. M. (2016). Changing climate and nutrient transfers: Evidence from high temporal resolution concentration-flow dynamics in headwater catchments. *Science of The Total Environment*, *548-549*, 325–339. http://dx.doi.org/10.1016/j.scitotenv.2015.12.086.

Ockenden, M. C., Hollaway, M. J., Beven, K. J., Collins, A. L., Evans, R., Falloon, P. D., … Haygarth, P. M. (2017). Major agricultural changes required to mitigate phosphorus losses under climate change. *Nature Communications*, *8*(1), http://dx.doi.org/10.1038/s41467-017-00232-0.

Ouellet, V., St-Hilaire, A., Dugdale, S. J., Hannah, D. M., Krause, S., & Proulx-Ouellet, S. (2020). River temperature research and practice: Recent challenges and emerging opportunities for managing thermal habitat conditions in stream ecosystems. *Science of the Total Environment*, *736*, 139679. https://doi.org/10.1016/j.scitotenv.2020.139679

Raymond, P. A., Saiers, J. E., & Sobczak, W. V. (2016). Hydrological and biogeochemical controls on watershed dissolved organic matter transport: Pulse-shunt concept. *Ecology*, *97*(1), 5–16. https://doi.org/10.1890/14-1684.1

Reaney, S. M., Mackay, E. B., Haygarth, P. M., Fisher, M., Molineux, A., Potts, M., & Benskin, C. M. H. (2019). Identifying critical source areas using multiple methods for effective diffuse pollution mitigation. *Journal of Environmental Management*, *250*, 109366. https://doi.org/10.1016/j.jenvman.2019.109366

Rode, M., Halbedel Nee Angelstein, S., Anis, M. R., Borchardt, D., & Weitere, M. (2016). Continuous in-stream assimilatory nitrate uptake from high-frequency sensor measurements. *Environmental Science & Technology*, *50*(11), 5685–5694. https://doi.org/10.1021/acs.est.6b00943

Rode, M., Wade, A. J., Cohen, M. J., Hensley, R. T., Bowes, M. J., Kirchner, J. W., … Jomaa, S. (2016). Sensors in the Stream: The High-Frequency Wave of the Present. *Environmental Science & Technology*, *50*(19), 10297–10307. http://dx.doi.org/10.1021/acs.est.6b02155.

Rose, L. A., Karwan, D. L., & Godsey, S. E. (2018). Concentration-discharge relationships describe solute and sediment mobilization, reaction, and transport at event and longer timescales. *Hydrological Processes*, *32*(18), 2829–2844. https://doi.org/10.1002/hyp.13235

Seneviratne, S. I., Nicholls, N., Easterling, D., Goodess, C. M., Kanae, S., Kossin, J., … Dahe, Q. (2012). Changes in climate extremes and their impacts on the natural physical. *Environment*, 109–230. https://doi.org/10.1017/cbo9781139177245.006.

Seymour, M. (2019). Rapid progression and future of environmental DNA research. *Communications Biology*, *2*, 80. https://doi.org/10.1038/s42003-019-0330-9

Smolders, E., Baetens, E., Verbeek, M., Nawara, S., Diels, J., & Verdievel, M. (2017). Internal loading and redox cycling of sediment

iron explain reactive phosphorus concentrations in lowland Rivers. *Environmental Science & Technology*, *51*, 2584–2592.

Thompson, S. E., Basu, N. B., Lascurain, J., Aubeneau, A., & Rao, P. S. C. (2011). Relative dominance of hydrologic versus biogeochemical factors on solute export across impact gradients. *Water Resources Research*, *47*(10), 1–20. https://doi.org/10.1029/2010wr009605.

Tickner, D., Opperman, J. J., Abell, R., Acreman, M., Arthington, A. H., Bunn, S. E., … Young, L. (2020). Bending the Curve of Global Freshwater Biodiversity Loss: An Emergency Recovery Plan. *BioScience*, *70*(4), 330–342. http://dx.doi.org/10.1093/biosci/biaa002.

Trauth, N., & Fleckenstein, J. H. (2017). Single discharge events increase reactive efficiency of the hyporheic zone. *Water Resources Research.*, *53*, 779–798. https://doi.org/10.1002/2016wr019488

Vannote, R. L., Minshall, G. W., Cummins, K. W., Sedell, J. R., & Cushing, C. E. (1980). The river continuum concept. *Canadian Journal of Fisheries and Aquatic Sciences*, *37*(1), 130–137. https://doi.org/10.1139/f80-017

Vorosmarty, C. J., Osuna, V. R., Koehler, D. A., Klop, P., Spengler, J. D., Buonocore, J. J., … Sanchez, R. (2018). Scientifically assess impacts of sustainable investments. *Science*, *359*(6375), 523–525. http://dx.doi.org/10.1126/science.aao3895.

Wang, L., & Burke, S. P. (2017). A catchment-scale method to simulating the impact of historical nitrate loading from agricultural land on the nitrate-concentration trends in the sandstone aquifers in the Eden Valley, UK. *Science of the Total Environment*, *579*, 133–148. https://doi.org/10.1016/j.scitotenv.2016.10.235

Wollheim, W. M., Bernal, S., Burns, D. A., Czuba, J. A., Driscoll, C. T., Hansen, A. T., … Wohl, E. (2018). River network saturation concept: factors influencing the balance of biogeochemical supply and demand of river networks. *Biogeochemistry*, *141*(3), 503–521. http://dx.doi.org/10.1007/s10533-018-0488-0.

Woodward, G., Bonada, N., Brown, L. E., Death, R. G., Durance, I., Gray, C., … Pawar, S. (2016). The effects of climatic fluctuations and extreme events on running water ecosystems. *Philosophical Transactions of the Royal Society B: Biological Sciences*, *371*(1694), 20150274http://dx.doi.org/10.1098/rstb.2015.0274.

Young, P., Pedregal, D., & Tych, W. (1999). Dynamic harmonic regression. *Journal of Forecasting*, *18*, 369–394.

Young, P., Taylor, C., Tych, W., & Pedregal, D. (2019). *The captain toolbox*. Lancaster University.

SUPPORTING INFORMATION

Additional supporting information may be found online in the Supporting Information section at the end of this article.

How to cite this article: Heathwaite AL, Bieroza M. Fingerprinting hydrological and biogeochemical drivers of freshwater quality. *Hydrological Processes*. 2021;35:e13973. https://doi.org/10.1002/hyp.13973